
PERGAMON

Journal of Quantitative Spectroscopy & Radiative Transfer 70 (2001) 675–695

Journal of Quantitative Spectroscopy & Radiative Transfer

www.elsevier.com/locate/jqsrt

Scattering properties of rutile pigments located eccentrically within microvoids

Jean-Claude Auger[a], Brian Stout[b], Rubén G. Barrera[c, *, 1], Fernando Curiel[a]

[a] *Centro de Investigación en Polímeros, COMEX, Marcos Achar Lobatón 2, 55885 Tepexpan, Estado de Mexico, Mexico*

[b] *L.O.E. UPRESA 6079, Faculté des Sciences et Techniques, Centre de Saint Jeróme, 13397 Marseilles Cedex 20, France*

[c] *Instituto de Física, UNAM, Apartado Postal 20-364, 01000 Mexico D.F., Mexico*

Abstract

We study the optical properties of opaque polymer pigmented coatings. The system consists of spherical rutile particles encapsulated in spherical microvoids embedded in a transparent polymer resin. The single-scattering properties of this system have been analyzed already, in case the rutile particle is located at the center of the microvoid . Here, we use a T-matrix approach to generalize and extend this analysis to the more realistic case when the rutile particles is located off-center within the microvoid. We also consider the multiple-scattering effects of a cluster composed by a collection of air bubbles with off-center rutile inclusions. Our calculations take into account the multiple scattering and the dependent-scattering processes of each pigment particle of the aggregate, using a new recursive T-matrix algorithm.

Keywords: Multiple-scattering; Off-center inclusions; T-matrix

1. Introduction

Since the last decade and due to the everyday larger availability and development of super computers, the field of scattering processes of electromagnetic waves in inhomogeneous media is in constant expansion. It is well known that the solution of Maxwell's equations for the scattered field from non-spherical objects or from even simple inhomogeneous systems, requires the implementation of elaborated numerical codes. Therefore, although the foundations of multiple scattering theory were set before the 1970s [1–3], its direct application has been

* Corresponding author. Tel.: +52-5622-5093; fax: +52-5616-1535.

E-mail address: rbarrera@fenix.ifisicacu.unam.mx (R.G. Barrera).

[1] Consultant at Centro de Investigación en Polímeros, COMEX.

0022-4073/01/$ - see front matter
PII: S0022-4073(01)00037-1

limited, to a great extent, by the capacity of computers for handling the existing numerical procedures. Nowadays, applications of the scattering theories of electromagnetic radiation, cover a wide range of interests, both in basic and in industrial research, in areas such as: astrophysics, atmospheric and material science, medical imagery analysis, and radar and I-R furtivity.

The work we present here is included in a research project for the coating industry, on white paints. A paint film can be described as an inhomogeneous medium composed of pigment particles embedded in a transparent polymer resin. Opacity (also called hiding power) is the property of the system to cover a substrate, to the human eye, when illuminated by light. In a white paint, opacity is the result of the multiple scattering of light by transparent pigment particles which enhances the reflectance of the otherwise transparent resin, yielding a diffuse angular distribution of the reflected light. At a local scale, a large opacity is related to a strong scattering efficiency of the pigment. This scattering efficiency is related to some intrinsic properties of the pigment particles, such as their shape and size, but also to system properties, like the relative index of refraction between the pigment and the surrounding resin. Due to its high refractive index (~ 2.8) and transparency in the visible range, rutile TiO_2 with an optimum size around 0.23 μm, has become the most efficient pigment in white paint formulation. At a global scale, opacity is proportional to the pigment volume concentration (PVC), since an increase in the PVC increases the amount of scattering centers and, consequently, the hiding power. However, at high PVC the reflectance of the film is no longer proportional to the PVC, showing a decrease in the scattering efficiency per particle. This effect is known as dependent scattering, and it also appears in the scattering from clusters. Since in a cluster the scattering efficiency per particle is reduced, in the production of white paints a special attention is given to processes or pigment surface treatments which help to minimize clustering.

However, a large part of the cost in the production of a white paint comes directly from the cost of TiO_2. As a consequence, there have been many efforts for trying to substitute rutile by a less expensive pigment, and air has been, since long, a good candidate. Microvoids encapsulated in a strong polyester resin, known commercially as Rhopaque, are already in the market. Although rutile is a more efficient light scatterer than air, one is not looking for the whole substitution of TiO_2 by microvoids, but rather for a partial substitution which could yield reasonable savings. There are also projects to manufacture vesiculated particles. These are transparent polymer micrometer particles filled with microvoids. In all these efforts, there is still the open question about the possibilities of improving the scattering efficiency of the microvoids. It has been argued [4], that the scattering efficiency of rutile could be improved by introducing the rutile particles inside the microvoids, because the contrast in the index of refraction between rutile and air is larger than the one between rutile and the resin. There is a very complete study [5] of the scattering properties of pigmented microvoid coatings, in which the TiO_2 spherical particles are located at the center of spherical microvoids, and the exact results for the scattering cross section of coated spheres [6] are used. It was found, that for pigments within microvoids whose size is much smaller than the wavelength of light, the scattering cross section per unit volume of the microvoid-pigment entity is, in general, much smaller than the corresponding one for the pigment and air bubble embedded separately in the resin. Nevertheless, the attention of this study was focused more on larger particles, where for specific combinations of geometrical and optical parameters of the pigment and the microvoid, an increase in the corresponding volumetric scattering efficiency of the microvoid-pigment entity

was found. This was called a synergetic effect. However, this effect occurred for sizes much larger than the optimum size of the TiO_2 particles to be useful in the coating industry, besides the unrealistic assumption of having the pigment right at the center of the microvoid.

The aim of this work is to present a study on the scattering properties of the TiO_2/microvoid system for a more general and realistic case, where the TiO_2 spherical inclusions are assumed to stick to the internal surface of the air bubble (off center of the sphere). Also, in order to take into account the dependent-scattering effects which occur in real paints, we present the study of the scattering properties of a cluster composed of a collection of air bubbles with off-center inclusions. The paper is organized as follows: Section 2 gives a short review of previous work, in Section 3, we present the T-matrix formalism which we develop to calculate the scattered field and the scattering cross section of an isolated sphere containing a spherical eccentric inclusion. Then, we extend these results by considering the scattering from an aggregate composed by several of these eccentric systems taking into account dependent-scattering effects. In Section 4, we present and discuss the results of our calculations, and finally Section 5 is devoted to our conclusion.

2. Previous work

The analytical derivations presented here are based on the T-matrix formalism originally developed by Waterman [7]. Its aim is the evaluation of the scattered field by an arbitrary-shaped particle by expressing the electric and magnetic fields in terms of the general solutions of the vector Helmholtz equation expanded in a spherical basis. Using the Extended Boundary Condition (EBC) also called the Null Field Approach one obtains a relation between the expansion coefficients of the scattered fields and those of the incident wave, through an infinite-dimensional matrix. This matrix is known as the T-matrix and can be calculated in terms of surface integrals of the fields at the scatterer boundary. In the case of a spherical geometry, these integrals are greatly simplified and the T-matrix approach becomes equivalent to Mie theory [8]. Numerical evaluations of the fields, using this formalism, have been possible because there is a natural cut-off for the infinite multipolar expansion of the fields. This cut-off depends on the size parameters of the system, that is, the modulus of the incident wave vector times the radius of the scatterer, and it is commonly admitted to be given by the Wiscombe criterium [9]. An additional advantage of the T-matrix formalism is that it can be systematically extended to solve the scattering problem from a collection of spherical particles located at arbitrary positions. The formalism for solving the electromagnetic scattering problem by a host sphere, containing a spherical eccentric inclusion, was first introduced by Fikioris [10], in the late 1970s. This approach was limited to the case in which the contrast between the refractive index of the inclusion and the host is sufficiently small. At the beginning of the last decade, Borghese [11] developed a more complete theory based on the single T-matrix approach. This formalism was applied to the evaluation of the differential scattering cross section of a metallic inclusion and an empty cavity within a host dielectric. Later on, Videen [12] developed an iterative procedure to solve the light scattering problem from a sphere with an inclusion of irregular shape. An application of this procedure to the case of a spherical inclusion was made by Ngo et al. [13]. Both of these approaches lifted the original restriction of sufficiently small contrast between the

refractive index of the host sphere and the inclusions. Furthermore, one of them allowed the solution of the more general problem in which the inclusion is located at a fixed distance from the origin, but it is randomly oriented. This requires an averaging procedure over all possible orientations of the inclusion, yielding average scattering parameters, where average means an orientational average. Now, the averaging over the orientations of the inclusion is equivalent to an average over all possible directions of the incident wave-vector, keeping the location of the inclusion fixed. This latter procedure turns out to be simpler and faster. However, the iterative procedure derived by Videen et al. [12] does not allow the analytical calculation of the average scattering parameters, which can be evaluated through a T-matrix formalism, and that are needed for a full characterization of the system. On the other hand, the T-matrix formalism provides us with the tools to solve not only the averaging problem of a single inclusion, but also to extend the formalism in order to obtain the solution of the multiple-scattering problem of a collection of host spheres with randomly oriented inclusions. But for this latter problem, the formulation of Borghese et al. [11] for an isolated eccentric system, does not consider all the possible localizations of the inclusion needed for the evaluation of the multiple-dependent scattering effect of several entities. Therefore, our purpose here is to derive a full T-matrix formulation for the eccentric system, in order to use it as an input in the multiple-scattering calculations for a cluster or a collection of host spheres with randomly oriented inclusions. We will do this, by taking as a guideline the formalism developed in the work of Ngo et al. [13], and then apply it to the above-mentioned case of rutile inclusions within air bubbles in resin.

3. Formalism

Let us consider an incident electric field of magnitude E_0 traveling as linearly polarized plane wave oscillating at frequency ω. The plane wave travels in a non-absorbing medium of refractive index N_0, and impinges on a system composed by a sphere centered at O_2, with radius a_2, and index of refraction N_2, which is located within a host sphere centered at O_1, with radius a_1 and refractive index N_1. The inclusion is located at a position denoted by $(r_0,\ \theta_0,\ \phi_0)$ in the spherical coordinate system of the host, and the wavelength of light in media 0, 1, and 2 will be denoted by λ_0, λ_1 and λ_2, respectively. Due to the spherical geometry of the two components of the system, it is found convenient to express the electric and magnetic fields in the different regions of space, in terms of the general solutions of the vector Helmholtz' equation expanded in a spherical-wave basis. Taking, first, the origin of the coordinate system at O_1, we write the electric field $\mathbf{E}$ as,

$$\mathbf{E}_{\mathrm{inc},1} = E_0 \sum_{\sigma=1}^{2} \sum_{n=1}^{\infty} \sum_{m=-n}^{n} a_{\sigma nm} \boldsymbol{\psi}^{(1)}_{\sigma nm,1}(k_0\mathbf{r}), \tag{1}$$

$$\mathbf{E}_{\mathrm{sca},1} = E_0 \sum_{\sigma=1}^{2} \sum_{n=1}^{\infty} \sum_{m=-n}^{n} f_{\sigma nm} \boldsymbol{\psi}^{(3)}_{\sigma nm,1}(k_0\mathbf{r}), \tag{2}$$

$$\mathbf{E}_{\mathrm{int},1} = E_0 \sum_{\sigma=1}^{2} \sum_{n=1}^{\infty} \sum_{m=-n}^{n} [e_{\sigma nm} \boldsymbol{\psi}^{(3)}_{\sigma nm,1}(k_1\mathbf{r}) + g_{\sigma nm} \boldsymbol{\psi}^{(4)}_{\sigma nm,1}(k_1\mathbf{r})], \tag{3}$$

where $\mathbf{r}$ denotes the position vector, $\mathbf{E}_{\mathrm{inc},1}$ is the incident plane wave of amplitude E_0, $\mathbf{E}_{\mathrm{sca},1}$, and $\mathbf{E}_{\mathrm{int},1}$ are the scattered and internal field, the subscript 1 denotes that the basis frame is R_1 with origin at O_1. By internal, we mean the region of space inside sphere 1 and outside sphere 2, and $k_0 = (2\pi N_0/\lambda_0)$ and $k_1 = (2\pi N_1/\lambda_1)$ are the magnitudes of the wave-vector in the matrix and in sphere 1, respectively. Here $a_{\sigma nm}$, $f_{\sigma nm}$, $e_{\sigma nm}$, and $g_{\sigma nm}$ are the expansion coefficients, and the spherical-wave basis is given by [14],

$$\boldsymbol{\psi}^{(i)}_{1nm}(kr,\theta,\phi) = \sqrt{\gamma_{nm}} \begin{pmatrix} 0 \\ \dfrac{\mathrm{i}m}{\sin\theta} z_n^{(i)}(kr) P_n^m(\cos\theta)\mathrm{e}^{\mathrm{i}m\phi} \\ -z_n^{(i)}(kr)\dfrac{\partial}{\partial\theta}[P_n^m(\cos\theta)]\mathrm{e}^{\mathrm{i}m\phi} \end{pmatrix} \begin{pmatrix} \hat{\mathbf{e}}_r \\ \hat{\mathbf{e}}_\theta \\ \hat{\mathbf{e}}_\phi \end{pmatrix} \tag{4}$$

and

$$\boldsymbol{\psi}^{(i)}_{2nm}(kr,\theta,\phi) = \sqrt{\gamma_{nm}} \begin{pmatrix} \dfrac{n(n+1)}{kr} z_n^{(i)}(kr) P_n^m(\cos\theta)\mathrm{e}^{\mathrm{i}m\phi} \\ \dfrac{1}{kr}\dfrac{\partial}{\partial r}[r\, z_n^{(i)}(kr)]\dfrac{\partial}{\partial\theta}[P_n^m(\cos\theta)]\mathrm{e}^{\mathrm{i}m\phi} \\ \dfrac{\mathrm{i}m}{kr\sin\theta}\dfrac{\partial}{\partial r}[r\, z_n^{(i)}(kr)] P_n^m(\cos\theta)\mathrm{e}^{\mathrm{i}m\phi} \end{pmatrix} \begin{pmatrix} \hat{\mathbf{e}}_r \\ \hat{\mathbf{e}}_\theta \\ \hat{\mathbf{e}}_\phi \end{pmatrix}, \tag{5}$$

where $\gamma_{nm} = (2n+1)(n-m)!/[4\pi n(n+1)(n-+m)!]$ is a normalization constant, P_n^m denotes the Legendre polynomials of second kind of order (n,m), and we follow the usual convention by taking $z_n^{(1)}(kr) \equiv j_n(kr)$, $z_n^{(3)}(kr) \equiv h_n^{(1)}(kr)$ and $z_n^{(4)}(kr) \equiv h_n^{(2)}(kr)$. Here $j_n(kr)$ is the spherical Bessel function, while $h_n^{(1)}(kr)$ and $h_n^{(2)}(kr)$ are the spherical Hankel functions of first and second kind, respectively, and we will be using SI units. Let us recall that $j_n(kr)$ are finite (regular) at the origin, while the waves with $h_n^{(1)}(kr)$ and $h_n^{(2)}(kr)$ describe outgoing and incoming spherical waves, respectively. Taking the origin of the coordinate system at O_2, the electric field in the region internal and external to sphere 2, can be written as,

$$\mathbf{E}_{\mathrm{int},2} = \sum_{\sigma=1}^{2}\sum_{n=1}^{\infty}\sum_{m=-n}^{n} p_{\sigma nm}\boldsymbol{\psi}^{(1)}_{\sigma nm,2}(k_2\mathbf{r}), \tag{6}$$

$$\mathbf{E}_{\mathrm{ext},2} = \sum_{\sigma=1}^{2}\sum_{n=1}^{\infty}\sum_{m=-n}^{n} [r_{\sigma nm}\boldsymbol{\psi}^{(3)}_{\sigma nm,2}(k_1\mathbf{r}) + t_{\sigma nm}\boldsymbol{\psi}^{(4)}_{\sigma nm,2}(k_1\mathbf{r})], \tag{7}$$

where the subscript 2 denotes that the basis frame is R_2 (which has its axes, respectively, parallel to those of R_1), with origin at O_2, $k_2 = (2\pi/\lambda_2)N_2$ is the magnitude of the wave-vector in sphere 2, and $p_{\sigma nm}$, $r_{\sigma nm}$, and $t_{\sigma nm}$ are the expansion coefficients.

One now applies boundary conditions at the interface of spheres 1 and 2, by demanding the continuity of tangential components of the electric and magnetic field. Since the electric and magnetic fields are related through Maxwell's equations, the corresponding expansions for the

magnetic field in the different regions of space do not actually add new expansion coefficients. Therefore, the boundary conditions at the interface of sphere 1 yield a set of four relations among the coefficients $a_{\sigma nm}$, $f_{\sigma nm}$, $e_{\sigma nm}$, and $g_{\sigma nm}$, and the boundary conditions at the interface of sphere 2 yield another set of four relations among the coefficients $p_{\sigma nm}$, $r_{\sigma nm}$, and $t_{\sigma nm}$. First, from this last relations one can eliminate the coefficients of the internal field of the inclusion ($p_{\sigma nm}$) getting a relation between the coefficients of the outgoing ($r_{\sigma nm}$) and the incoming waves ($t_{\sigma nm}$), which can be written as, $r_{\sigma nm} = Q_n^{\sigma} t_{\sigma mn}$, where Q_n^{σ} are given in Appendix A. Obviously, the internal field of the host, $\mathbf{E}_{\mathrm{int},1}$, and the external field of the inclusion, $\mathbf{E}_{\mathrm{ext},2}$, are the same but expressed in two different coordinate systems. It is then necessary to use the translation addition theorem for a spherical basis in order to express the coefficients of the internal field of the host ($e_{\sigma nm}, g_{\sigma nm}$) in terms of the coefficients of the external field of the inclusion ($r_{\sigma nm}, t_{\sigma nm}$). In this case, the general form of the addition theorem for $r > r_0$ is given by relation (B.1), see also [15]:

$$\boldsymbol{\psi}_{1nm,2}^{(q)} = \sum_{\nu=1}^{\infty} \sum_{\mu=-\nu}^{\nu} [\mathrm{Rg} A_{nm}^{\nu\mu(q)} \boldsymbol{\psi}_{1\nu\mu,1}^{(q)} + \mathrm{Rg} B_{nm}^{\nu\mu(q)} \boldsymbol{\psi}_{2\nu\mu,1}^{(q)}] \quad q = 3,4, \tag{8}$$

$$\boldsymbol{\psi}_{2nm,2}^{(q)} = \sum_{\nu=1}^{\infty} \sum_{\mu=-\nu}^{\nu} [\mathrm{Rg} B_{nm}^{\nu\mu(q)} \boldsymbol{\psi}_{1\nu\mu,1}^{(q)} + \mathrm{Rg} A_{nm}^{\nu\mu(q)} \boldsymbol{\psi}_{2\nu\mu,1}^{(q)}] \quad q = 3,4, \tag{9}$$

where Rg denotes regular part, and the explicit expressions for the coefficients $A_{nm}^{\nu\mu(q)}$ and $B_{nm}^{\nu\mu(q)}$ are given in Appendix A, where one can see that $A_{nm}^{\nu\mu(q)}$ and $B_{nm}^{\nu\mu(q)}$ contain the spherical function $z_n^{(q)}(kr)$, which is chosen with the same convention as above. Here, it is assumed that the series expansions of the translation addition theorem are uniformly convergent. Therefore, one can truncate the series at $\nu = \nu_{\mathrm{MAX}}$ assuming that the resulting error is small enough if ν_{MAX} is sufficiently large. Since the coefficients $A_{nm}^{\nu\mu(3)}$, $B_{nm}^{\nu\mu(3)}$ and $A_{nm}^{\nu\mu(4)}$, $B_{nm}^{\nu\mu(4)}$ contain the spherical Hankel functions $h_n^{(1)}(kr)$ and $h_n^{(2)}(kr)$, and their regular part is $j_n(kr)$, we have $\mathrm{Rg} A_{nm}^{\nu\mu(4)} = \mathrm{Rg} A_{nm}^{\nu\mu(3)} = A_{nm}^{\nu\mu(1)}$ and $\mathrm{Rg} B_{nm}^{\nu\mu(4)} = \mathrm{Rg} B_{nm}^{\nu\mu(3)} = B_{nm}^{\nu\mu(1)}$.

One now substitutes Eqs. (8) and (9) into Eq. (7) for the external field of the inclusion $\mathbf{E}_{\mathrm{ext},2}$ and identifies the resulting expansion with the one for internal field of the host sphere $\mathbf{E}_{\mathrm{int},1}$, getting a relation between the coefficients ($r_{\sigma nm}$, $t_{\sigma nm}$) and ($e_{\sigma nm}$, $g_{\sigma nm}$). If one goes back to the four equations obtained from the boundary conditions at the interface of sphere 1, and uses the relations between ($r_{\sigma nm}$, $t_{\sigma nm}$) and ($e_{\sigma nm}$, $g_{\sigma nm}$) and $r_{\sigma nm} = Q_n^{\sigma} t_{\sigma mn}$, one obtains four equations which relate the coefficients $a_{\sigma nm}$ of the incident field, the coefficients $f_{\sigma mn}$ of the scattered field and the coefficients $t_{\sigma\nu\mu}$ of the internal field. This can be finally written as,

$$a_{2nm}\psi_n(k_0 a_1) + f_{2nm}\xi_n^{(1)}(k_0 a_1) = \sum_{\nu} \sum_{\mu} [t_{1\nu\mu} B_{\nu\mu}^{nm(1)} Z_{\nu n}^{(a)} + t_{2\nu\mu} A_{\nu\mu}^{nm(1)} Z_{\nu n}^{(b)}], \tag{10}$$

$$a_{2nm}\psi_n'(k_0 a_1) + f_{2nm}\xi_n'^{(1)}(k_0 a_1) = \frac{k_0}{k_1} \sum_{\nu} \sum_{\mu} [t_{1\nu\mu} B_{\nu\mu}^{nm(1)} Z_{\nu n}^{(c)} + t_{2\nu\mu} A_{\nu\mu}^{nm(1)} Z_{\nu n}^{(d)}], \tag{11}$$

$$a_{1nm}\psi_n'(k_0a_1) + f_{1nm}\xi_n'^{(1)}(k_0a_1) = \sum_{\nu}\sum_{\mu}[t_{1\nu\mu}A_{\nu\mu}^{nm(1)}Z_{\nu n}^{(c)} + t_{2\nu\mu}B_{\nu\mu}^{nm(1)}Z_{\nu n}^{(d)}], \tag{12}$$

$$a_{1nm}\psi_n(k_0a_1) + f_{1nm}\xi_n^{(1)}(k_0a_1) = \frac{k_0}{k_1}\sum_{\nu}\sum_{\mu}[t_{1\nu\mu}A_{\nu\mu}^{nm(1)}Z_{\nu n}^{(a)} + t_{2\nu\mu}B_{\nu\mu}^{nm(1)}Z_{\nu n}^{(b)}], \tag{13}$$

where $\psi_n(x)=xj_n(x)$, $\xi_n^{(1)}=xh_n^{(1)}(x)$, the prime denotes a derivative with respect to the argument and $Z_{\nu n}^{(a)}$, $Z_{\nu n}^{(b)}$, $Z_{\nu n}^{(c)}$, and $\bar{Z}_{\nu n}^{(d)}$ are given in Appendix A.

From these relations one can obtain the T-matrix coefficients of the total system (host plus inclusion sphere). One first eliminates the expansion coefficients (f_{1nm}, f_{2nm}) of the scattered field in order to express the expansion coefficients (a_{1nm}, a_{2nm}) of the incident field in terms of the expansion coefficients $(t_{1\nu\mu}, t_{2\nu\mu})$ of the internal field. This is expressed in terms of a matrix relation which is then inverted to get a relationship between the coefficients $(t_{1\nu\mu}, t_{2\nu\mu})$ of the internal field and those of the incident field. This relationship can be written succinctly as, $\mathbf{t} = \bar{\mathbf{M}}^{-1} \cdot \mathbf{a}$, where $\mathbf{t}$ and $\mathbf{a}$ (in bold) denote column vector. Now, from these same relations (Eqs. (10)–(13)), one eliminates the coefficients (a_{1nm}, a_{2nm}) in order to obtain a matrix relation between the expansion coefficients of the scattering field (f_{1nm}, f_{2nm}) and the expansion coefficients of the internal field $(t_{1\nu\mu}, t_{2\nu\mu})$, that is, $\mathbf{f} = \bar{\mathbf{D}} \cdot \mathbf{t}$. Finally, by combining the $\bar{\mathbf{M}}^{-1}$ and $\bar{\mathbf{D}}$ matrices, one can express directly the coefficients of the scattered field $\mathbf{f}$ in terms of the coefficients of the incident field $\mathbf{a}$, through a T-matrix relation,

$$\mathbf{f} = \bar{\mathbf{D}} \cdot \bar{\mathbf{M}}^{-1} \cdot \mathbf{a} \equiv \bar{\mathbf{T}} \cdot \mathbf{a}, \tag{14}$$

where $\bar{\mathbf{T}}$ is the T-matrix of the eccentric–sphere system. The explicit expressions for the components of the matrices $\bar{\mathbf{M}}$ and $\bar{\mathbf{D}}$ are given in Appendix A.

3.1. Multiple-scattering equations

Let us consider a collection of N randomly located spheres with radius a_i and complex refractive indexes n_s^i $(i=1,N)$. The center of each sphere O_i is defined in a principal coordinate system O by a position vector $\mathbf{r}_i$ and the relative position vector between two arbitrary spheres i and j is denoted by $\mathbf{r}_{ij}$. Due to the superposition principle, the total electric field $\mathbf{E}_{\text{sca}}^{\text{T}}$ scattered by the cluster, is equal to the sum of the fields scattered by each of the individual sphere, that is, $\mathbf{E}_{\text{sca}}^{\text{T}} = \sum_i \mathbf{E}_{\text{sca}}^{i(N)}$. First we define the local field $\mathbf{E}_{\text{loc}}^{i(N)}$ at the ith sphere as the sum, at ith, of applied incident field $\mathbf{E}_{\text{inc}}^{i}$ plus the fields $\mathbf{E}_{\text{sca}}^{j(N)}$ scattered by all the other spheres. The fields are now expanded in a spherical vector wave functions. However, while the incident field is naturally expanded in the principal coordinate system O, the fields scattered from each of the jth spheres are expanded in the coordinate system O_j. Therefore, in order to express both terms in the coordinate system of the ith sphere, one should use the translational addition theorem

(relations (B.2) and (B.3)), and write,

$$\mathbf{E}_{\mathrm{loc}}^{i(N)} = \mathrm{Rg}\boldsymbol{\psi}^{(3)t}(k_0|\mathbf{r}-\mathbf{r}_i|)\cdot\bar{\mathbf{J}}^{(i,0)}\cdot\mathbf{a} + \sum_{\substack{j=1\\ j\neq i}}^{N}\mathrm{Rg}\boldsymbol{\psi}^{(3)t}(k_0|\mathbf{r}-\mathbf{r}_i|)\cdot\bar{\mathbf{H}}^{(i,j)}\cdot\mathbf{f}^{j(N)}, \tag{15}$$

where the superscript t means transpose (row vector), $\bar{\mathbf{J}}^{(i,0)}$ and $\bar{\mathbf{H}}^{(i,j)}$ are the translation matrices for the incident and the scattered fields, respectively, and they are given in Appendix B. Here $\mathbf{f}^{j(N)}$ is the column vector whose components are the expansion coefficients of the electric field scattered by the jth sphere in the cluster. Using the definition of the single T-matrix $\bar{\mathbf{T}}^{i(1)}$ of the ith sphere, and the definition of the local field (Eq. (15)), one can write a set of N coupled-linear equations for the scattering coefficients ($i = 1,\ldots,N$),

$$\mathbf{f}^{i(N)} = \bar{\mathbf{T}}^{i(1)}\left[\bar{\mathbf{J}}^{(i,0)}\cdot\mathbf{a} + \sum_{\substack{j=1\\ j\neq i}}^{N}\bar{\mathbf{H}}^{(i,j)}\cdot\mathbf{f}^{j(N)}\right] = \bar{\mathbf{T}}^{i(N)}\cdot\bar{\mathbf{J}}^{(i,0)}\cdot\mathbf{a}, \tag{16}$$

where $\bar{\mathbf{T}}^{i(N)}$ is the ith N-scatterer T-matrix, which includes all the information about the multiple-scattering effects due to the presence of the $N-1$ other scatterers. Using Eq. (16), one gets a set of N coupled-linear equations whose unknowns are the N-scattered T-matrix coefficients of each individual sphere, that is,

$$\bar{\mathbf{T}}^{i(N)} = \bar{\mathbf{T}}^{i(1)}\left[\bar{\mathbf{I}} + \sum_{\substack{j=1\\ j\neq i}}^{N}\bar{\mathbf{H}}^{(i,j)}\cdot\bar{\mathbf{T}}^{j(N)}\cdot\bar{\mathbf{J}}^{(j,i)}\right]. \tag{17}$$

This system can be solved using different kinds of procedures, such as, the direct matrix inversion , the order of scattering method, or iterative and recursive algorithms. A detailed description of these methods are available in the current literature, see for example [16–19]. One of the main advantages of this formalism is that each scatterer is characterized through its single T-matrix $\bar{\mathbf{T}}^{i(1)}$, with the only restriction of having an external spherical geometry. Thus, they can be either metallic, dielectric, coated, multi-layered, or even spherical particles containing one or more spherical inclusions.

3.2. Extension of the recursive T-matrix algorithm

Here we first review briefly the Recursive T-matrix Algorithm (RTMA) introduced by Chew [20] for scalar waves and extended to the electromagnetic case by Tzeng and Fung [21], and then extend the concept of N-centered T-matrix developed by Mackowski [18] to the calculation of the scattering properties of a collection of spheres with randomly oriented eccentric inclusions.

In the RTMA procedure, the presence of the Nth sphere in the cluster acts as a perturbation on the $N-1$ previous scatterers, modifying their scattering properties. It can be shown that the recurrence relations of this algorithm are given by,

$$\bar{\mathbf{T}}^{N(N)} \cdot \bar{\mathbf{J}}^{(N,0)} = \left[\bar{\mathbf{I}} - \bar{\mathbf{T}}^{N(1)} \sum_{i=1}^{N-1} \cdot \bar{\mathbf{H}}^{(N,i)} \cdot \bar{\mathbf{T}}^{i(N-1)} \cdot \bar{\mathbf{J}}^{(i,0)} \bar{\mathbf{H}}^{(0,N)} \right]^{-1} \times \bar{\mathbf{T}}^{N(1)} \left[\bar{\mathbf{J}}^{(N,0)} + \sum_{i=1}^{N-1} \cdot \bar{\mathbf{H}}^{(N,i)} \cdot \bar{\mathbf{T}}^{i(N-1)} \cdot \bar{\mathbf{J}}^{(i,0)} \right], \tag{18}$$

$$\bar{\mathbf{T}}^{i(N)} \cdot \bar{\mathbf{J}}^{(i,0)} = \bar{\mathbf{T}}^{i(N-1)} \bar{\mathbf{J}}^{(i,0)} [\bar{\mathbf{I}} + \bar{\mathbf{H}}^{(0,N)} \cdot \bar{\mathbf{T}}^{N(N)} \cdot \bar{\mathbf{J}}^{(N,0)}] \quad i \neq N. \tag{19}$$

The algorithm has two steps: first, one needs to evaluate the multiple T-matrix $\bar{\mathbf{T}}^{N(N)}$ of the Nth scatterer as a function of the $\bar{\mathbf{T}}^{i(N-1)}$ matrices of each constituent of the $(N-1)$ cluster Eq. (18). Then, the individual multiple-scattering T-matrices $\bar{\mathbf{T}}^{i(N)}$ for a cluster with N scatterers are evaluated from the previous individual multiple-scattering T-matrices $\bar{\mathbf{T}}^{i(N-1)}$ and the $\bar{\mathbf{T}}^{N(N)}$ matrix Eq. (19). Nevertheless, the numerical implementation of this algorithm encounters convergence problems due to the necessary cut-off of the $\bar{\mathbf{J}}^{(i,0)}$ and $\bar{\mathbf{J}}^{(N,0)}$ matrices associated with the translation of the incident plane wave which has non-negligible components up to infinite order. To overcome this truncation problem, some modifications to the RTMA procedure, based on the phase-shift formalism, have been proposed [22]. Unfortunately these modifications have not proven to be successful in all types of clusters . Furthermore, convergence problems might also arise whenever the perturbation $\Delta\bar{\mathbf{T}}^{i(N)} \equiv \bar{\mathbf{T}}^{i(N)} - \bar{\mathbf{T}}^{i(N-1)}$, due to the presence of the Nth sphere, is not small. Therefore, in order to cope with some of these problems, we extend here the RTMA algorithm, using the N-centered T-matrix concept $\bar{\tau}_N^{(i,j)}$ introduced by Mackowski [18] who pointed out that a formal matrix inversion of the scattering Eq. (16) could be written as:

$$\begin{bmatrix} \mathbf{f}^{1(N)} \\ \mathbf{f}^{2(N)} \\ \vdots \\ \mathbf{f}^{N(N)} \end{bmatrix} = \begin{bmatrix} \bar{\tau}_N^{(1,1)} & \bar{\tau}_N^{(1,2)} & \cdots & \bar{\tau}_N^{(1,N)} \\ \bar{\tau}_N^{(2,1)} & \bar{\tau}_N^{(2,2)} & \cdots & \bar{\tau}_N^{(2,N)} \\ \vdots & \vdots & \ddots & \vdots \\ \bar{\tau}_N^{(N,1)} & \bar{\tau}_N^{(N,2)} & \cdots & \bar{\tau}_N^{(N,N)} \end{bmatrix} \begin{bmatrix} \bar{\mathbf{J}}^{(1,0)} \cdot \mathbf{a} \\ \bar{\mathbf{J}}^{(2,0)} \cdot \mathbf{a} \\ \vdots \\ \bar{\mathbf{J}}^{(N,0)} \cdot \mathbf{a} \end{bmatrix}. \tag{20}$$

Using relation (16) in Eq. (20) one expresses the N-scattered T-matrix $\bar{\mathbf{T}}^{i(N)}$ of the ith sphere in terms of the N-centered T-matrix $\bar{\tau}_N^{(i,j)}$. These latter matrices are defined through the relation:

$$\bar{\mathbf{T}}^{i(N)} = \sum_{j=1}^{N} \bar{\tau}_N^{(i,j)} \cdot \bar{\mathbf{J}}^{(j,i)}, \quad i = 1, \ldots, N. \tag{21}$$

Since the scattering properties of the cluster are given by $\bar{\mathbf{T}}^{i(N)}$, these properties will then be fully specified once all the N-centered T-matrix $\bar{\tau}_N^{(i,j)}$ are determined. Below we propose an analytical procedure towards this aim.

One starts by substituting the corresponding expression for $\bar{\mathbf{T}}^{i(N-1)}$, given by Eq. (21), into Eq. (18), and then using the relations $\bar{\mathbf{J}}^{(i,N)} = \bar{\mathbf{J}}^{(i,j)} \cdot \bar{\mathbf{J}}^{(j,N)}$ and $\bar{\mathbf{H}}^{(i,N)} = \bar{\mathbf{J}}^{(i,j)} \cdot \bar{\mathbf{H}}^{(j,N)}$ to write,

$$\bar{\mathbf{T}}^{N(N)} = \left[\bar{\mathbf{I}} - \bar{\mathbf{T}}^{N(1)} \cdot \sum_{i=1}^{N-1} \bar{\mathbf{H}}^{(N,i)} \cdot \sum_{j=1}^{N-1} \bar{\tau}_{N-1}^{(i,j)} \cdot \bar{\mathbf{H}}^{(j,N)}\right]^{-1} \bar{\mathbf{T}}^{N(1)} \times \left[\bar{\mathbf{I}} + \sum_{i=1}^{N-1} \bar{\mathbf{H}}^{(N,i)} \cdot \sum_{j=1}^{N-1} \bar{\tau}_{N-1}^{(i,j)} \cdot \bar{\mathbf{J}}^{(j,N)}\right]. \tag{22}$$

A comparison of this expression with the corresponding one given by Eq. (21), in terms of the matrices $\bar{\tau}_N^{(N,i)}$, leads to the identification of two recursive relations for the centered T-matrices $\bar{\tau}_N^{(N,N)}$ and $\bar{\tau}_N^{(N,j)}$, given by

$$\bar{\tau}_N^{(N,N)} = \left[\bar{\mathbf{I}} - \bar{\mathbf{T}}^{N(1)} \sum_{i=1}^{N-1} \bar{\mathbf{H}}^{(N,i)} \cdot \sum_{j=1}^{N-1} \bar{\tau}_{N-1}^{(i,j)} \cdot \bar{\mathbf{H}}^{(j,N)}\right]^{-1} \cdot \bar{\mathbf{T}}^{N(1)}, \tag{23}$$

$$\bar{\tau}_N^{(N,j)} = \bar{\tau}_N^{(N,N)} \cdot \left[\bar{\mathbf{I}} + \sum_{i=1}^{N-1} \bar{\mathbf{H}}^{(N,i)} \cdot \bar{\tau}_{N-1}^{(i,j)}\right], \quad j \neq N. \tag{24}$$

To obtain analogous recursive relations for the matrices $\bar{\tau}_N^{(i,j)}$ and $\bar{\tau}_N^{(j,N)}$, one substitutes the corresponding expressions for $\bar{\mathbf{T}}^{i(N-1)}$ and $\bar{\mathbf{T}}^{N(N)}$ in terms of $\bar{\tau}_{N-1}^{(i,j)}$ and $\bar{\tau}_N^{(N,j)}$, as given by Eq. (21), into Eq. (19). After some rearrangement of terms one gets,

$$\bar{\mathbf{T}}^{i(N)} = \sum_{j=1}^{N-1} \bar{\tau}_{N-1}^{(i,j)} \cdot \bar{\mathbf{J}}^{(j,i)} \cdot \bar{\mathbf{H}}^{(i,N)} \cdot \left(\sum_{k=1}^{N-1} \bar{\tau}_N^{(N,k)} \cdot \bar{\mathbf{J}}^{(k,i)} + \bar{\tau}_N^{(N,N)} \cdot \bar{\mathbf{J}}^{(N,i)}\right) + \sum_{j=1}^{N-1} \bar{\tau}_{N-1}^{(i,j)} \cdot \bar{\mathbf{J}}^{(j,i)}, \tag{25}$$

which after some algebra, yields

$$\bar{\mathbf{T}}^{i(N)} = \sum_{j=1}^{N-1} \left[\bar{\tau}_{N-1}^{(i,j)} + \sum_{k=1}^{N-1} \bar{\tau}_{N-1}^{(i,k)} \cdot \bar{\mathbf{H}}^{(k,N)} \cdot \bar{\tau}_N^{(N,j)}\right] \cdot \bar{\mathbf{J}}^{(i,k)} + \sum_{j=1}^{N-1} \bar{\tau}_{N-1}^{(i,j)} \cdot \bar{\mathbf{H}}^{(j,N)} \cdot \bar{\tau}_N^{(N,N)} \cdot \bar{\mathbf{J}}^{(N,i)}. \tag{26}$$

Finally, using in the above equation the expression for $\bar{\mathbf{T}}^{i(N)}$ in terms of $\bar{\tau}_N^{(i,j)}$, one can identify the two last recursive relations for the N-centered T-matrices $\bar{\tau}_N^{(i,j)}$ and $\bar{\tau}_N^{(i,N)}$, which can be written as

$$\bar{\tau}_N^{(i,j)} = \bar{\tau}_{N-1}^{(i,j)} + \sum_{k=1}^{N-1} \bar{\tau}_{N-1}^{(i,k)} \cdot \bar{\mathbf{H}}^{(k,N)} \cdot \bar{\tau}_N^{(N,j)} \quad j \neq N, \tag{27}$$

$$\bar{\tau}_N^{(i,N)} = \sum_{j=1}^{N-1} \bar{\tau}_{N-1}^{(i,j)} \cdot \bar{\mathbf{H}}^{(j,N)} \cdot \bar{\tau}_N^{(N,N)}, \quad i \neq N. \tag{28}$$

In conclusion, the recursive relations (23), (24), (27) and (28) provide the evaluation of all the N-centered T-matrices $\bar{\tau}_N^{(i,j)}$ of an ensemble of particles with symmetrical geometry. Once all the $\bar{\tau}_N^{(i,j)}$ matrices are determined, the scattered fields $\mathbf{f}^{i(N)}$ can be calculated from Eqs. (21) and (16), and the problem is solved. The initial values in the recursive algorithm can be obtained, solving system (17) for two spheres problem, in which the N-centered T-matrices $\bar{\tau}_N^{(1,1)}$, $\bar{\tau}_N^{(1,2)}$, $\bar{\tau}_N^{(2,1)}$ and $\bar{\tau}_N^{(2,2)}$ can be easily identified from the expressions for $\bar{\mathbf{T}}^{1(2)}$ and $\bar{\mathbf{T}}^{2(2)}$.

$$\bar{\tau}_N^{(1,1)} = [\bar{\mathbf{I}} - \bar{\mathbf{T}}^{1(1)} \cdot \bar{\mathbf{H}}^{(1,2)} \cdot \bar{\mathbf{T}}^{2(1)} \cdot \bar{\mathbf{H}}^{(2,1)}]^{-1} \cdot \bar{\mathbf{T}}^{1(1)}, \tag{29}$$

$$\bar{\tau}_N^{(1,2)} = \bar{\tau}_N^{(1,1)} \cdot \bar{\mathbf{H}}^{(1,2)} \cdot \bar{\mathbf{T}}^{2(1)}, \tag{30}$$

$$\bar{\tau}_N^{(2,2)} = [\bar{\mathbf{I}} - \bar{\mathbf{T}}^{2(1)} \cdot \bar{\mathbf{H}}^{(2,1)} \cdot \bar{\mathbf{T}}^{1(1)} \cdot \bar{\mathbf{H}}^{(1,2)}]^{-1} \cdot \bar{\mathbf{T}}^{2(1)}, \tag{31}$$

$$\bar{\tau}_N^{(2,1)} = \bar{\tau}_N^{(2,2)} \cdot \bar{\mathbf{H}}^{(2,1)} \cdot \bar{\mathbf{T}}^{1(1)}. \tag{32}$$

The main advantage of this approach is that the recursion relations do not involve $\bar{\mathbf{J}}^{(i,0)}$ matrices and as a consequence they are free from their truncation problem evoked in the previous paragraph. Also each $\bar{\tau}_N^{(i,j)}$ matrices start with an ordinary one-particle transfer matrix of type $\bar{\mathbf{T}}^{i(1)}$ and end with a transfer matrix of type $\bar{\mathbf{T}}^{j(1)}$. As these transfer matrices have a natural truncation arising from their physical size parameter, the $\bar{\tau}_N^{(i,j)}$ will always have their dimension limited to the same multipolarity.

3.3. Optical properties

The study of the optical properties of a system made of spherical scatterers with an eccentric inclusion, embedded in an otherwise homogeneous medium, requires an adequate treatment of the multiple scattering phenomenon. These spherical scatterers can be either isolated or in clusters, and are dispersed in the matrix with different filling fractions and with different statistical correlations. One of the main ingredients in almost any approach to the multiple scattering problem are the scattering properties of the isolated scatterers. These scattering properties are given by quantities like the differential scattering cross section and the total extinction and scattering cross sections. In case of a system with anisotropic spherical scatterers with random orientations, one would require the orientational averages of both the extinction and scattering cross

sections. The connection between these concepts and the T-matrix is that there is a well-defined relationship between all these cross sections and the elements of the T-matrix. For example, the relation between the extinction cross section of an isolated scatterer and the elements of its T-matrix is,

$$C_{\text{ext}} = -\frac{1}{k^2}\text{Re}[\mathbf{a}^t(\bar{\mathbf{T}}\mathbf{a})^*], \tag{33}$$

while the orientational average of the extinction cross section $\langle C_{\text{ext}}\rangle$ for anisotropic scatterers can be calculated as [23],

$$\langle C_{\text{ext}}\rangle = -\frac{2\pi}{k^2}\text{Tr}[\bar{\mathbf{T}}], \tag{34}$$

Here, k is the amplitude of the incident wave vector, * is complex conjugate, $\langle\ldots\rangle$ denotes the orientational average over all incident angles and polarization states, and Tr denotes trace. On the other hand, the average extinction cross section for a cluster of N spheres can be expressed in terms of the T-matrix $\bar{\mathbf{T}}^{i(N)}$ of each of its components. For example, Mackowski [24] and Fuller [25] have shown that the total average extinction cross section $\langle C_{\text{ext}}^{\text{T}}\rangle$ of the cluster is simply given by,

$$\langle C_{\text{ext}}^{\text{T}}\rangle = \sum_{i=1}^{N}\langle C_{\text{ext}}^{i(N)}\rangle = -\frac{2\pi}{k^2}\sum_{i=1}^{N}\text{Tr}[\bar{\mathbf{T}}^{i(N)}], \tag{35}$$

while the differential scattering cross section for one isolated scatterer can be written as [26],

$$\frac{\text{d}C_{\text{sca}}}{\text{d}\Omega} = \frac{1}{k_0^2}[|F_\theta|^2 + |F_\phi|^2] \tag{36}$$

with

$$F_\theta \equiv \sum_{n=1}^{\infty}(-i)^n\sum_{m=-n}^{n}\sqrt{\gamma_{nm}}(f_{1nm}\pi_n^m(\cos\theta) + f_{2nm}\tau_n^m(\cos\theta))\text{e}^{\text{i}m\phi},$$

$$F_\phi \equiv \sum_{n=1}^{\infty} -(-i)^{n+1}\sum_{m=-n}^{n}\sqrt{\gamma_{nm}}(f_{2nm}\pi_n^m(\cos\theta) + f_{1nm}\tau_n^m(\cos\theta))\text{e}^{\text{i}m\phi},$$

where $\pi_n^m(\cos\theta) = \frac{m}{\sin\theta}P_n^m(\cos\theta)$ and $\tau_n^m(\cos\theta) = \frac{\partial}{\partial\theta}P_n^m(\cos\theta)$ are the angular functions.

4. Results and discussion

The code implemented and used for this study has been rigorously checked and tested. The calculations were performed on an Alpha processor and numerical results, on various clusters of different sizes and geometries, were compared and found in good agreement with the ones available in the literature. We present here only the most relevant results taken from a more complete analysis of the system. Since we are interested on the optical properties of paint films as seen by the human eye, we have used in all our calculations a wavelength of 0.56 μm, which is the wavelength at which the spectral sensitivity of a standard observer attains its maximum.

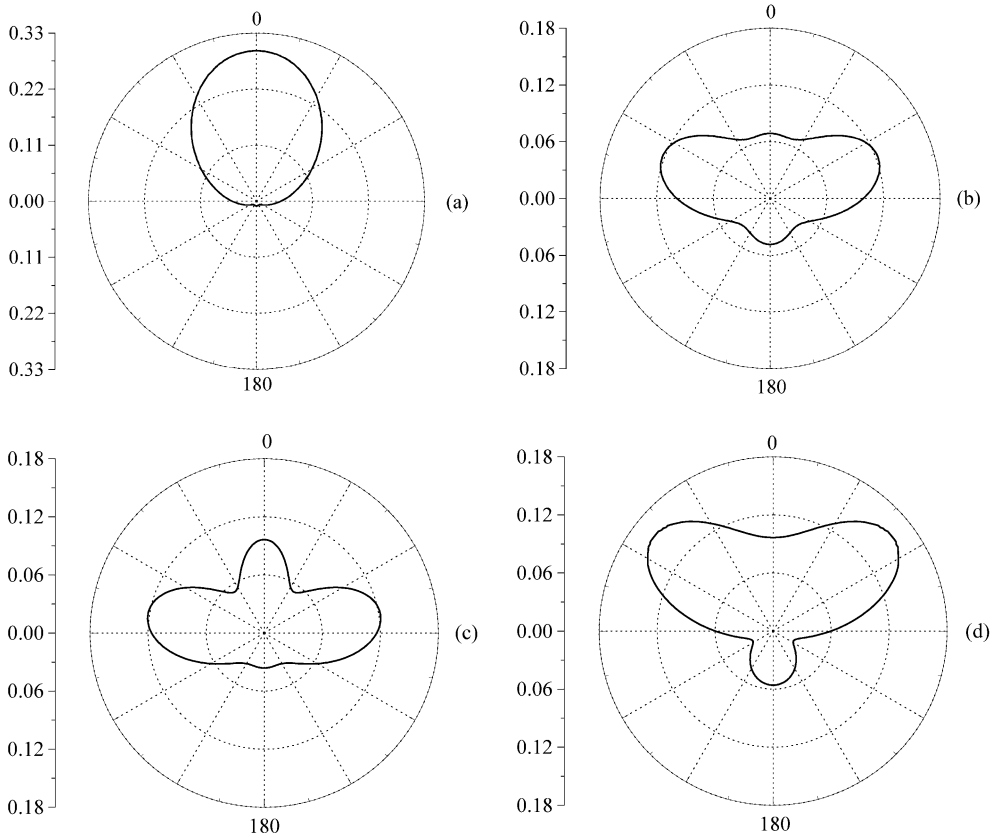

Fig. 1. Normalized differential scattering cross sections as function of the scattering angles: $0 \leqslant \theta_{sca} \leqslant 180^\circ$, $\phi_{sca} = 90^\circ$. The incident light is unpolarized, the wave-vector parallel to the O_z axis. Radii of TiO_2 sphere and microvoid are $a_1 = 0.15$ μm and $a_2 = 0.096$ μm, respectively. (a) TiO_2 embedded in resin. In (b), (c) and (d) TiO_2 sphere is inside the microvoid such as: ($r_0 = 0$, $\theta_0 = 0$, $\phi_0 = 0$), ($r_0 = r_m$, $\theta_0 = 0$, $\phi_0 = 0$) and ($r_0 = r_m$, $\theta_0 = \pi$, $\phi_0 = 0$), respectively.

The indexes of refraction of the microvoids, the rutile pigment and the surrounding medium (resin) are taken as real and equal to 1.0, 2.8 and 1.5, respectively. First, we present results related to the scattering properties of an isolated system composed by a microvoid with an eccentric spherical rutile inclusion and later on we discuss the dependent-scattering properties of a collection of these anisotropic entities.

4.1. Scattering by microvoids with an eccentric spherical inclusion

Before looking at the change in scattering power as the rutile inclusion is brought into the microvoid, we start by looking at the effect of its eccentric location in the angular distribution of the scattered light. For this, we calculate and compare the angular distribution of the differential scattering cross section of the isolated system for different locations (r_0, θ_0, ϕ_0) of the inclusion within the microvoid. Some results of these calculations are shown in Fig. 1, where the radius

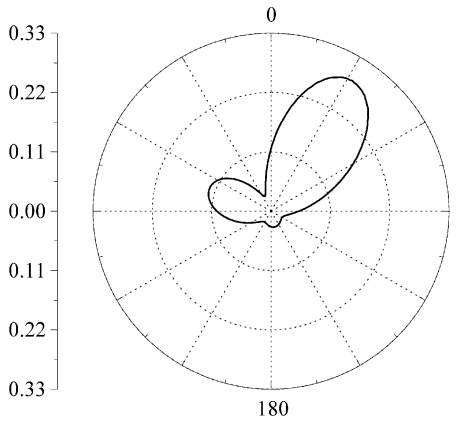

Fig. 2. Same as Fig. 1 with the scattering angles: $0 \leqslant \theta_{sca} \leqslant 180°$, $\phi_{sca} = 90°$ and $180 \leq \theta_{sca} \leqslant 0°$, $\phi_{sca} = 270°$. The position of the TiO_2 sphere is $(r_0 = r_m,\ \theta_0 = \pi/2, \phi_0 = \pi/2)$.

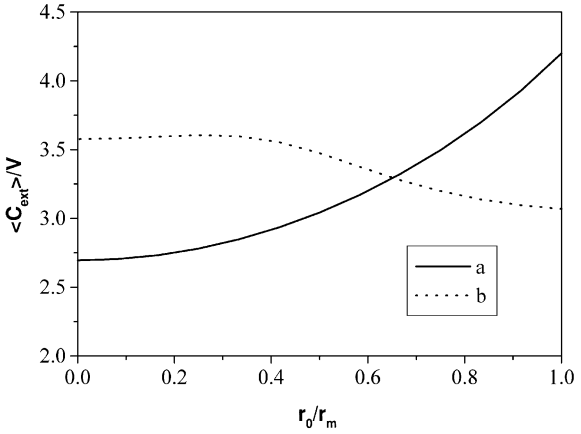

Fig. 3. Volumetric average extinction cross sections, in μm^{-1}, as functions of the distance of the pigment from the center of the host sphere to its maximum value r_m. (a) $a_1 = 0.15$ μm, $a_2 = 0.096$ μm, and $r_m = 0.054$ μm. (b) $a_1 = 0.51$ μm, $a_2 = 0.43$ μm, and $r_m = 0.07$ μm.

of the air bubble and the rutile pigment are kept constant and equal to $a_1 = 0.15$ μm and $a_2 = 0.096$ μm, respectively. Light is taken unpolarized, the azimuthal angle of scattering is fixed at $\phi_{sca} = 90°$, and the wave-vector of the incident field is taken parallel to the O_z axis of the host sphere. As a consequence, an azimuthal symmetry is kept as long as the inclusion stays on this axis. Also, the integral of the differential cross section over all solid angles is normalized to 1. In Fig. 1 we show the angular distribution of the differential cross section when the pigment (a) is embedded in resin, when (b) is located at the center of the microvoid, and when located at (c) $(r_0 = r_m,\ \theta_0 = 0,\ \phi_0 = 0)$, and (d) $(r_0 = r_m,\ \theta_0 = \pi,\ \phi_0 = 0)$, where $r_m = 0.054$ μm is the maximum radial position of the inclusion. In the two last locations the inclusion is stuck to the upper (c) and bottom (d) sides of the internal interface of the host sphere. In curve (a) one sees the typical strong scattering in forward direction predicted by the Mie theory. When the pigment is located at the center of the microvoid (b) the angular distribution broadens. Now, when one compares curves (c) and (d) with (b), one observes an enhancement in the intensity of the scattered light in the same direction as the off-center location of the inclusion. It seems like the off-center direction of the inclusion is indicating the direction in which the intensity of the scattered light is enhanced. To test the generality of this assessment, in Fig. 2 we show the angular distribution of the scattered light when the inclusion is located off the O_z axis, at $(r_0 = r_m, \theta_0 = \pi/2, \phi_0 = \pi/2)$. In this case, the azimuthal symmetry of the angular distribution is broken but one still sees that the intensity of scattered light is greatly enhanced on the side of the microvoid where the inclusion is located. Then, one concludes that the angular distribution of the scattering field is strongly linked to the location of the pigment within the microvoid, being enhanced along the off-center direction of the inclusion.

The displacement of the inclusion within the microvoid also has an influence on the scattering properties of the isolated system. In Fig. 3, we show the normalized average of the extinction

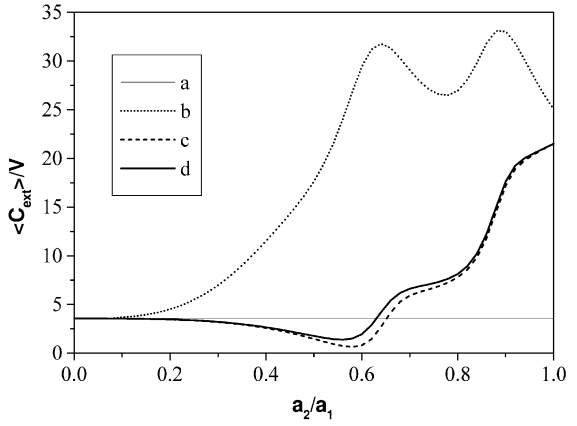

Fig. 4. Volumetric average extinction cross sections, in μm^{-1}, as functions of a_2/a_1 with $a_1 = 0.15$ μm. (a) air microvoid alone. (b) TiO_2 and microvoid separated in the resin. (c) TiO_2 at the center of the microvoid. (d) TiO_2 stuck to the microvoid internal surface ($r_0 = r_m$).

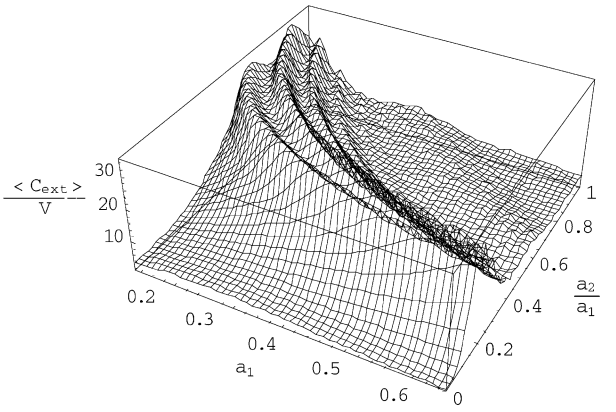

Fig. 5. Volumetric average extinction cross sections, in μm^{-1}, as functions of a_1 and a_2/a_1, for TiO_2 and microvoid as separated entities in resin.

cross section, over all incident angles and polarization states (orientational average), as a function of the distance of the pigment from the center of the host sphere to its maximum value r_m. Curve (a) corresponds to a system where $a_1 = 0.15$ μm, $a_2 = 0.096$ μm, and $r_m = 0.054$ μm, while in curve (b) $a_1 = 0.51$ μm, $a_2 = 0.43$ μm, and $r_m = 0.07$ μ m. One can see that the displacement of the pigment from the center to the edge of the host sphere can lead to either an increase or a decrease in the magnitude of average extinction cross section. For the system in panel (a), the average extinction cross section increases by a factor 1.56 between its minimum at $r_0 = 0$ and its maximum at $r_0 = r_m$. On the other hand, for the system in curve (b) the magnitude of the average extinction cross section decreases by a factor 0.15 for the same translation from the center to the edge. In this latter case, the maximum occurs at an intermediate distance between the center and the edge while the minimum is at r_m. Therefore, one concludes that the behavior of the average extinction cross section of the isolated system, as a function of the size parameter and the location of the inclusion, is non-monotonic.

After this succinct analysis of the effect of the pigment location on the scattering properties of the isolated system, we now look at the changes on the average extinction cross section when the pigment is brought into the microvoids. We recall that one of our objectives is to test if there is an improvement in the scattering properties of rutile inclusions when the contrast in the index of refraction is increased by bringing them inside air bubbles. To look at this we calculate the extinction cross section per unit volume (volumetric cross section) for three different systems: In system 1 we consider that both, the rutile spheres and the microvoids are embedded in resin and they behave as independent scatterers. In system 2 the rutile spheres are located at the center of the microvoids while in system 3 the rutile spheres are stuck to the internal face of the microvoids with random orientations. This latter system is supposed to give a more realistic description of an actual system. In Fig. 4 we show, the average volumetric

extinction cross sections for systems 1, 2 and 3, respectively. These cross sections are plotted as functions of a_2/a_1 for $a_1 = 0.15$ μm. The values $a_2/a_1 = 0$ and 1 correspond, respectively, to a microvoid without pigment and a pigment in resin with the same size of the air bubble. For a better understanding of the figure we have added curve (a), which is the volumetric extinction cross section of the air microvoid alone. The major observation of this calculation is that in the chosen range of size parameters, the volumetric extinction cross section of system 1 (curve(b)) is always larger than in systems 2 and 3 (curves (c) and (d), respectively). This simply means that rutile is a less efficient scatterer when it is located inside the air bubbles than when it is outside. One can also see that for small values of a_2/a_1, the presence of the pigment does not perturb the scattering properties of the microvoid. On the other hand, when a_2/a_1 is close to 1, the extinction of the system is dominated by the extinction of rutile. There are a couple of things we should point out about this figure. The first one is the strong decrease in the extinction cross sections in curves (c) and (d) at ($a_2/a_1 = 0.58$), although the decrease in (d) is not as pronounced. With such a low value of the extinction cross section, one might say that the system behaves as "invisible" to the incident wave, where by this we mean the remanent of a phenomenon found out by Kerker [28], for the case of coated spheres and in the limit of small size parameters (Rayleigh scattering). Under this condition and for specific combinations of values of the relative refractive indexes and radii, it can be shown that the induced dipole in the host sphere has the same amplitude but opposite direction as the one induced dipole in the inclusion. Thus, the total dipole moment is null and there is simply no scattering. The second observation is that at $a_2/a_1 = 0.64$, the microvoid alone scatters more than the system with the pigment located at the center but less than when it is located at its maximum position r_m. Based on this observation we evaluated the average extinction cross section as a function of r_0. It was found that for $r_0 = 0.04$ μm, the extinction of the eccentric system was equal to that of the microvoid alone, leading to the conclusion that at this location, the rutile pigment (with a filling fraction of 0.26) is "invisible" to the incident wave. Therefore, in the same way as the centered inclusion can lead to an "invisible" system for certain combinations of size parameters, here we show that an eccentric location of the inclusion can lead to interference effects such that the inclusions might become "invisible" inside the microvoid.

To check if the main conclusion of the previous calculations continues to hold for a different choice of size parameters, we have evaluated the extinction cross section for the three systems mentioned above, for values of a_1 and a_2 in the range $0.15 < a_1 < 0.65$ μm and $0 \leqslant a_2 \leqslant a_1$. It was found that the values of the volumetric extinction cross section of the centered and eccentric systems was quite similar, but always smaller than when the TiO_2 pigment is outside the microvoid. In Figs. 5 and 6 we show, in a 3D plot, the results for the volumetric extinction cross section as a function of a_1 and a_1/a_2 for systems 1 and 3. One can see that the conclusions reached above about the loss of scattering power of the rutile inclusions inside an air bubble also hold for this extended choice of parameters. Also, the highest value of the volumetric extinction cross section is always attained at the optimum size of the rutile sphere in resin.

4.2. Dependent scattering by microvoids containing an eccentric TiO_2 spherical inclusion

Since dependent scattering processes are also important in a paint film, the recursive procedure introduced in the previous section was used to evaluate its effects on clusters composed by a

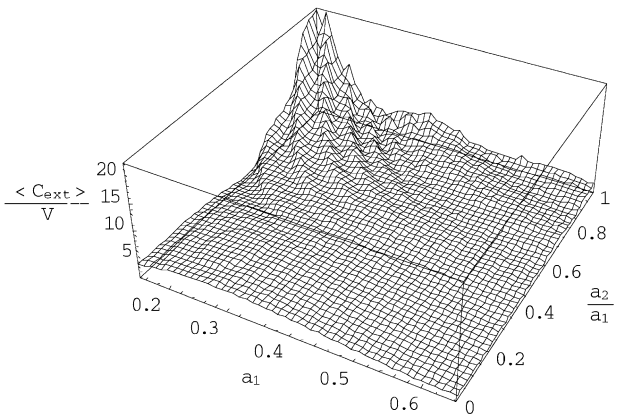

Fig. 6. Same as Fig. 5 for TiO_2 stuck to the microvoid internal surface ($r_0 = r_m$).

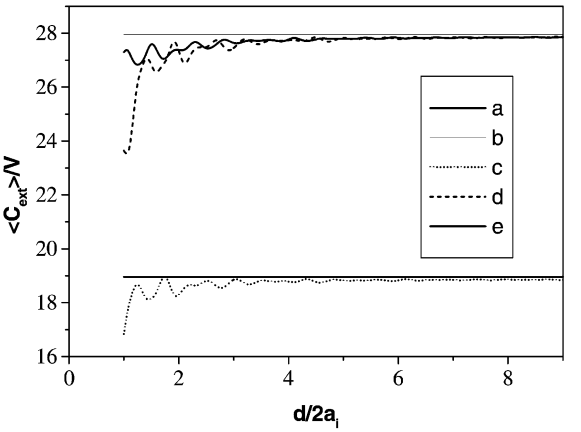

Fig. 7. Volumetric average extinction cross sections, in μm^{-1}, of clusters with seven scattering spheres as functions of the distance d between each spheres and the origin. The radii of the TiO_2 spheres and microvoids are $a_2 = 0.96\ \mu m$ and $a_1 = 0.15\ \mu m$, respectively. (a) and (b): independent-scattering calculations for eccentric and centered pigments. (c), (d) and (e): dependent-scattering calculations with the inclusions at the center of the microvoid, closest and the farthest from the origin of the aggregate, respectively.

microvoid system containing randomly oriented eccentric inclusion of rutile. In Fig. 7, we show the average volumetric extinction cross sections of three different aggregates of seven spheres as a function of the radial distance d between the central sphere and each of its six other constituents. Each aggregate is built up of seven scatters, one at the origin and the others located at positions $(0,0,d)$, $(0,0,-d)$, $(d,0,0)$, $(-d,0,0)$, $(0,d,0)$ and $(0,-d,0)$. Each scatterer is made of rutile pigment with radius $a_2 = 0.96\ \mu m$, and located in a microvoid of radius $a_1 = 0.15\ \mu m$. The results for the different relative locations of the pigment inside each microvoid are labeled with different letters. In plot (c), the inclusion is at the center, while in plots (d) and (e) the inclusion is located at the closest and the farthest positions from the central sphere in the aggregate. For a better understanding of the results, the total volumetric extinction cross sections of a system composed of independent scattering spheres for eccentric and centered pigments were added in plots (a) and (b), respectively. The parameters were chosen so that an isolated system with a centered pigment scatters less than the one with an eccentric position. One can see that as it is expected, at long distances between the constituents of a same cluster the dependent and independent cross sections are identical. When these distances decrease, dependent scattering becomes predominant leading to a decrease of the total extinction cross section. Appearance of oscillations should come from interferences and resonant modes due to the symmetrical geometry chosen for the clusters. When all scatterers are in contact (case of a compact cluster), curve (d) undergoes a higher decrease than curve (e) because it corresponds to the case where the TiO_2 pigments inside the microvoid are closer, leading to a stronger effect of dependent scattering.

5. Conclusion

In this paper, we have derived the general T-matrix formulations for an isolated system composed of a dielectric sphere containing an eccentric dielectric spherical inclusion. We also have presented a new recursive procedure to solve the coupled linear equations for multiple scattering problem. We applied these formalisms to the study of the optical properties of microvoids containing eccentric TiO_2 pigments. It is shown that the scattering efficiency of TiO_2 pigment is not improved when it is introduced into a microvoid.

Acknowledgements

The authors acknowledge Eduardo Nahmad for the support given to this work.

Appendix A. Expressions of the $\bar{\mathbf{M}}$ and $\bar{\mathbf{D}}$ matrices

In this appendix we write, as a reference, the explicit form of several expressions used in the text.

$$Q_n^1 = \left[\frac{k_1\xi_n'^{(2)}(k_1r_2)\psi_n(k_2r_2) - k_2\xi_n^{(2)}(k_1r_2)\psi_n'(k_2r_2)}{k_2\xi_n^{(1)}(k_1r_2)\psi_n'(k_2r_2) - k_1\xi_n'^{(1)}(k_1r_2)\psi_n(k_2r_2)}\right],$$

$$Q_n^2 = \left[\frac{k_1\xi_n^{(2)}(k_1r_2)\psi_n'(k_2r_2) - k_2\xi_n'(2)(k_1r_2)\psi_n(k_2r_2)}{k_2\xi_n'^{(1)}(k_1r_2)\psi_n(k_2r_2) - k_1\xi_n^{(1)}(k_1r_2)\psi_n'(k_2r_2)}\right], \tag{A.1}$$

and

$$Z_{\nu n}^{(a)} = [Q_\nu^1\xi_n^{(1)}(k_1a_1) + \xi_n^{(2)}(k_1a_1)],$$

$$Z_{\nu n}^{(b)} = [Q_\nu^2\xi_n^{(1)}(k_1a_1) + \xi_n^{(2)}(k_1a_1)],$$

$$Z_{\nu n}^{(c)} = [Q_\nu^1\xi_n'^{(1)}(k_1a_1) + \xi_n'^{(2)}(k_1a_1)],$$

$$Z_{\nu n}^{(d)} = [Q_\nu^2\xi_n'^{(1)}(k_1a_1) + \xi_n'^{(2)}(k_1a_1)]. \tag{A.2}$$

The general expressions for the $\bar{\mathbf{M}}$ and $\bar{\mathbf{D}}$ matrices are given by the following relations:

$$\bar{\mathbf{M}} = \begin{bmatrix} \bar{M}_{\nu\mu}^{nm(1,1)} & \bar{M}_{\nu\mu}^{nm(1,2)} \\ \bar{M}_{\nu\mu}^{nm(2,1)} & \bar{M}_{\nu\mu}^{nm(2,2)} \end{bmatrix} \quad \text{and} \quad \bar{\mathbf{D}} = \begin{bmatrix} \bar{D}_{\nu\mu}^{nm(1,1)} & \bar{D}_{\nu\mu}^{nm(1,2)} \\ \bar{D}_{\nu\mu}^{nm(2,1)} & \bar{D}_{\nu\mu}^{nm(2,2)} \end{bmatrix}. \tag{A.3}$$

$$\bar{M}_{\nu\mu}^{nm(1,1)} = A_{\nu\mu}^{nm(1)} \left[\frac{Z_{\nu n}^{(c)} \xi_n^{(1)}(k_0 a_1) - (k_0/k_1) Z_{\nu n}^{(a)} \xi_n'^{(1)}(k_0 a_1)}{\psi_n'(k_0 a_1) \xi_n^{(1)}(k_0 a_1) - \psi_n(k_0 a_1) \xi_n'^{(1)}(k_0 a_1)} \right],$$

$$\bar{M}_{\nu\mu}^{nm(1,2)} = B_{\nu\mu}^{nm(1)} \left[\frac{Z_{\nu n}^{(d)} \xi_n^{(1)}(k_0 a_1) - (k_0/k_1) Z_{\nu n}^{(b)} \xi_n'^{(1)}(k_0 a_1)}{\psi_n'(k_0 a_1) \xi_n^{(1)}(k_0 a_1) - \psi_n(k_0 a_1) \xi_n'^{(1)}(k_0 a_1)} \right],$$

$$\bar{M}_{\nu\mu}^{nm(2,1)} = B_{\nu\mu}^{nm(1)} \left[\frac{Z_{\nu n}^{(a)} \xi_n'^{(1)}(k_0 a_1) - (k_0/k_1) Z_{\nu n}^{(c)} \xi_n^{(1)}(k_0 a_1)}{\psi_n(k_0 a_1) \xi_n'^{(1)}(k_0 a_1) - \psi_n'(k_0 a_1) \xi_n^{(1)}(k_0 a_1)} \right],$$

$$\bar{M}_{\nu\mu}^{nm(2,2)} = A_{\nu\mu}^{nm(1)} \left[\frac{Z_{\nu n}^{(b)} \xi_n'^{(1)}(k_0 a_1) - (k_0/k_1) Z_{\nu n}^{(d)} \xi_n^{(1)}(k_0 a_1)}{\psi_n(k_0 a_1) \xi_n'^{(1)}(k_0 a_1) - \psi_n'(k_0 a_1) \xi_n^{(1)}(k_0 a_1)} \right], \tag{A.4}$$

$$\bar{D}_{\nu\mu}^{nm(1,1)} = A_{\nu\mu}^{nm(1)} \left[\frac{(k_0/k_1) Z_{\nu n}^{(a)} \psi_n'(k_0 a_1) - Z_{\nu n}^{(c)} \psi_n(k_0 a_1)}{\xi_n^{(1)}(k_0 a_1) \psi_n'(k_0 a_1) - \xi_n'^{(1)}(k_0 a_1) \psi_n(k_0 a_1)} \right],$$

$$\bar{D}_{\nu\mu}^{nm(1,2)} = B_{\nu\mu}^{nm(1)} \left[\frac{(k_0/k_1) \bar{\mathbf{Z}}_{\nu n}^{(b)} \psi_n'(k_0 a_1) - Z_{\nu n}^{(d)} \psi_n(k_0 a_1)}{\xi_n^{(1)}(k_0 a_1) \psi_n'(k_0 a_1) - \xi_n'^{(1)}(k_0 a_1) \psi_n(k_0 a_1)} \right],$$

$$\bar{D}_{\nu\mu}^{nm(2,1)} = B_{\nu\mu}^{nm(1)} \left[\frac{(k_0/k_1) Z_{\nu n}^{(c)} \psi_n(k_0 a_1) - Z_{\nu n}^{(a)} \psi_n'(k_0 a_1)}{\xi_n'^{(1)}(k_0 a_1) \psi_n(k_0 a_1) - \xi_n^{(1)}(k_0 a_1) \psi_n'(k_0 a_1)} \right],$$

$$\bar{D}_{\nu\mu}^{nm(2,2)} = A_{\nu\mu}^{nm(1)} \left[\frac{(k_0/k_1) Z_{\nu n}^{(d)} \psi_n(k_0 a_1) - Z_{\nu n}^{(b)} \psi_n'(k_0 a_1)}{\xi_n'^{(1)}(k_0 a_1) \psi_n(k_0 a_1) - \xi_n^{(1)}(k_0 a_1) \psi_n'(k_0 a_1)} \right], \tag{A.5}$$

where $A_{nm}^{\nu\mu(q)}$ and $B_{nm}^{\nu\mu(q)}$ are defined in Appendix B.

Appendix B. Translation theorem

The expressions of the translational theorem for spherical wave functions are:

$$\boldsymbol{\psi}^{(q)\mathrm{t}}(k_0|\mathbf{r} - \mathbf{r}_i|) = \boldsymbol{\psi}^{(q)\mathrm{t}}(k_0|\mathbf{r} - \mathbf{r}_k|) \cdot \bar{\mathbf{J}}^{(k,i)}, \quad r > r_{ik}, \tag{B.1}$$

$$\mathrm{Rg}\boldsymbol{\psi}^{(q)\mathrm{t}}(k_0|\mathbf{r} - \mathbf{r}_i|) = \mathrm{Rg}\boldsymbol{\psi}^{(q)\mathrm{t}}(k_0|\mathbf{r} - \mathbf{r}_k|) \cdot \bar{\mathbf{J}}^{(k,i)}, \quad \forall r_{ik}, \tag{B.2}$$

$$\boldsymbol{\psi}^{(q)\mathrm{t}}(k_0|\mathbf{r} - \mathbf{r}_i|) = \mathrm{Rg}\boldsymbol{\psi}^{(q)\mathrm{t}}(k_0|\mathbf{r} - \mathrm{r}_k|) \cdot \bar{\mathbf{H}}^{(k,i)}, \quad r < r_{ik}, \tag{B.3}$$

where $q = 1, 2$ and $\bar{\mathbf{J}}^{(k,i)}$ and $\bar{\mathbf{H}}^{(k,i)}$ are the translational matrices which can be written

as:

$$\bar{\mathbf{J}}^{(k,i)} = \begin{bmatrix} \mathrm{Rg}A_{nm}^{\nu\mu(q)} & \mathrm{Rg}B_{nm}^{\nu\mu(q)} \\ \mathrm{Rg}B_{nm}^{\nu\mu(q)} & \mathrm{Rg}A_{nm}^{\nu\mu(q)} \end{bmatrix} \quad \text{and} \quad \bar{\mathbf{H}}^{(k,i)} = \begin{bmatrix} A_{nm}^{\nu\mu(q)} & B_{nm}^{\nu\mu(q)} \\ B_{nm}^{\nu\mu(q)} & A_{nm}^{\nu\mu(q)} \end{bmatrix} \tag{B.4}$$

The $A_{nm}^{\nu\mu(q)}$ and $B_{nm}^{\nu\mu(q)}$ are the translation coefficients needed for the transformation from the ith to the kth coordinate system. They depend on the position vector $\mathbf{r}_{ki}$ between the two spheres and the amplitude of the wave-vector of the medium in which they are. They can be derived from scalar translational matrices coefficients [27], $\beta_{n,m}^{\nu,\mu}$ and $\alpha_{n,m}^{\nu,\mu}$ expended in terms of the $j_n(kr)$ and $h_n^{(1)}(kr)$, respectively. Then one can use the relations between vector and scalar coefficients derived by Mackowski. In terms of our chosen normalization for the spherical-wave basis, Eq. (4) and Eq. (25) have the following expressions:

$$\begin{aligned} RgA_{nm}^{\nu\mu(1)} = {} & \frac{1}{2}\sqrt{\frac{1}{\nu(\nu+1)n(n+1)}}[2\ \mu\mathrm{m}\beta_{n,m}^{\nu,\mu} \\ & + \sqrt{(n-m)(n+m+1)(\nu-\mu)(\nu+\mu+1)}\beta_{n,m+1}^{\nu,\mu+1} \\ & + \sqrt{(n+m)(n-m+1)(\nu+\mu)(\nu-\mu+1)}\beta_{n,m-1}^{\nu,\mu-1}] \end{aligned} \tag{B.5}$$

$$\begin{aligned} RgB_{nm}^{\nu\mu(1)} = {} & -\mathrm{i}\frac{1}{2}\sqrt{\frac{2\nu+1}{2\nu-1}\frac{1}{\nu(\nu+1)n(n+1)}}[2m\sqrt{(\nu-\mu)(\nu+\mu)}\beta_{n,m}^{\nu-1,\mu} \\ & + \sqrt{(n+m)(n+m+1)(\nu-\mu)(\nu-\mu-1)}\beta_{n,m+1}^{\nu-1,\mu+1} \\ & - \sqrt{(n+m)(n-m+1)(\nu+\mu)(\nu+\mu-1)}\beta_{n,m-1}^{\nu-1,\mu-1}] \end{aligned} \tag{B.6}$$

The $A_{nm}^{\nu\mu(3)}$ and $B_{nm}^{\nu\mu(3)}$ coefficients are found from relations (B.5) and (B.6) replacing the $\beta_{n,m}^{\nu,\mu}$ scalar matrix coefficients by the $\alpha_{n,m}^{\nu,\mu}$.

References

[1] Chandrasekhar S. Radiative transfer. New York: Dover, 1960.
[2] Frisch U. Propagation des ondes en milieu aléatoire et les équations stochastisques. Annales d'Astrophysique 1966;29:645–82.
[3] Frisch U. Annales d'Astrophysique 1966;30:565–601.
[4] Wick ZW, Jones FN, Pappas PS. Organic coatings: science and technology. Vol. 1. New York: Wiley; 1992.
[5] Ross W. Theoretical computation of light scattering power: comparison between TiO_2 and air bubbles. J Paint Technol 1971;43(563):50–65.
[6] Kerker M, Cooke D, Ross W. Pigmented microvoid coatings: theoretical study of three models. Paint Res Inst 1975;47(603):33–41.
[7] Waterman P. Symmetry unitary and geometry in electromagnetic scattering. Phys Rev D 1971;3(4):825–39.

[8] Bohren CF, Huffman DR. Absorption and scattering of light by small particles. New York: Wiley-Interscience; 1983.
[9] Wiscombe W. Improve Mie scattering algorithms. Appl Opt 1980;19(9):1505–9.
[10] Fikioris U. J Opt Soc Am 1979;69:1359.
[11] Borghese F, Denti P, Saija R. Optical properties of spheres containing a spherical eccentric inclusion. J Opt Soc Am A 1992;9(8):1327–35.
[12] Videen G, Ngo D, Chylek P, Pinnick R. Light scattering from a sphere with an irregular inclusion. J Opt Soc Am A 1995;12(5):922–8.
[13] Ngo D, Videen G, Chylek P. A FORTRAN code for the scattering of EM waves by a sphere with a nonconcentric spherical inclusion. Comput Phys Commun 1996;1077:94–112.
[14] Tsang L, Kong J, Shin R. Theory of microwave remote sensing. New York: Wiley; 1985.
[15] Stein S. Addition theorems for spherical wave functions. Quart Appl Math 1961;19(1):15–24.
[16] Borghese F, Denti P, Saija R, Toscano G. Multiple electromagnetic scattering from a cluster of sphere I theory. Aerosol Sci Technol 1984;4:227–35.
[17] Hamid A. Electromagnetic scattering by an arbitrary configuration of dielectric spheres. Can J Phys 1990;68:1419–28.
[18] Mackowski D, Mishchenko M. Calculation of the T-matrix and the scattering matrix for ensembles of spheres. J Opt Soc Am A 1996;13(11):2266–78.
[19] Xu Y. Electromagnetic scattering by an aggregate of sphere. Appl Opt 1995;34(21):4573–88.
[20] Chew W. Waves and Fields in Inhomogeneous Media, Series on Electromagnetic Waves. New York: IEEE Press; 1990.
[21] Tzeng Y, Fung A. T-matrix approach to multiple scattering of EM waves from N-spheres. J Electromagn Waves Appl 1994;8(1):61–84.
[22] Holler S, Auger JC, Stout B, Pan Y, Bottiger J, Chang RK, Videen G. Observations and calculations of light scattering from clusers of spheres. Appl Opt 2000;39(36):6873–87.
[23] Mishchenko M, Travis L, Mackowski D. T-matrix computations of light scattering by nonspherical particles: a review. JQSRT 1996;55(5):535–75.
[24] Mackowski D. Calculation of total cross sections of multiple-sphere clusters. J Opt Soc Am A 1994;11(11):2851–61.
[25] Fuller K. Scattering and absorption cross sections of compounded spheres: I theory for external aggregation. J Opt Soc Am A 1994;11(12):3251–60.
[26] Van de Hulst HC. Light scattering by small particles. New York: Dover; 1957.
[27] Chew W. Recurrence relations for three-dimensional scalar addition theorem. J Electromagn Waves Appl 1992;6(2):133–42.
[28] Kerker M. Invisible bodies. J Opt Soc Am A 1975;65(4):376–9.